

# Integrations of Slanted Silicon Nanostructures on 3D Microstructures and Its Application in Surface Enhanced Raman Spectroscopy

Zhida Xu<sup>1</sup>, Jing Jiang<sup>1</sup>, Manas Ranja Gartia<sup>1</sup>, Gang Logan Liu<sup>1\*</sup>

**Abstract** – Black silicon with slanted nanopillar array on planar and microstructure was produced for surface-enhanced Raman spectroscopy (SERS). The angle dependence of etching angle and nanopillar slanted angle was investigated with scanning electron microscopy.

**Index Terms** - Black Silicon, Angle-Controllable Nanopillar, Slanted Reaction Ion Etching, Polarized SERS.

## I. INTRODUCTION

Black silicon is a semiconductor material whose surface is modified with micro or nanostructures to become highly absorptive, thus appears black. Its application in SERS and fluorescence enhancement has been demonstrated before.[1,2] In this work, we fabricated black silicon with slanted nanopillar array on both planar and 3D micro and meso scale structures produced by a high-throughput mask-less oblique-angle plasma etching process. By integrating nanopillars on inverse silicon micro-pyramid array devices, we further improved the SERS enhancement property of this optimized commercial SERS substrate by several folds even when using 70% less noble metal coating. We investigated the length gradient dependence and asymmetric properties of SERS effects for slanted nanopillar with polarized excitation. This versatile and angle-controllable nanopillar fabrication and monolithic 3D nano-micro-meso integration method provides new dimensions for production and optimization of SERS and other nanophotonic sensors.

## II. INTEGRATION OF NANOPILLAR ONTO NON-PLANAR MICRO-STRUCTURED SILICON SURFACES

To demonstrate that the nanopillar can be produced on 3D non-planar silicon surface, especially on existing microstructures, we chose three kinds of silicon microstructures including positive pyramids, inverse pyramidal pits and sharp AFM tip. Scanning electron microscopy (SEM) images of these microscale surfaces before (insets of Fig. 1a, c, and e) and after (Fig. 1b, d, and e) the monolithic integration of slanted silicon nanopillars are shown in Fig. 1. The positive microscale pyramids are on the surface of commercial solar cells, produced by KOH anisotropic etching of silicon (Fig. 1a and b). The inverse pyramidal pits are on surface of Klarite SERS substrate (Renishaw), produced by photolithography and KOH anisotropic etching (Fig. 1c and d). Figure 1(e) and (f) show nanopillars formed on an AFM silicon cantilever tip. All these surfaces turn black after the nanopillars are formed

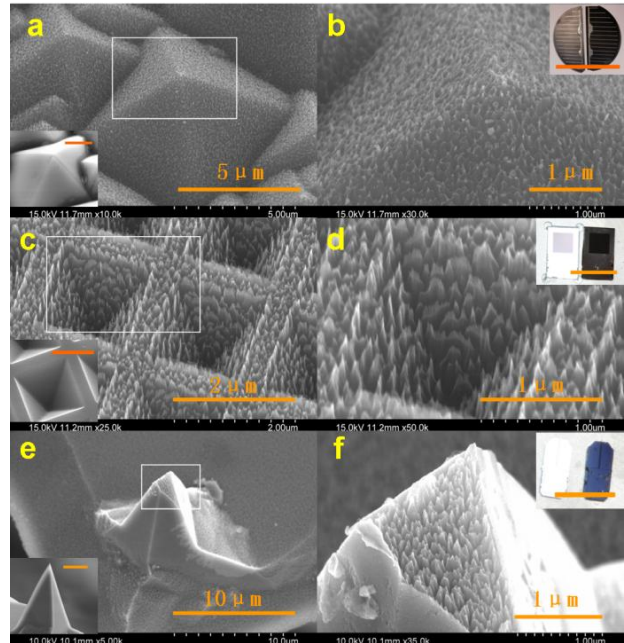


Figure 1 (a) and (b) Nanopillar forest made on silicon pyramids. (c) and (d) Nanopillar forest made on inverted pyramids on silicon (black Klarite). (e) and (f) Nanopillar forest made on silicon AFM tip. For each row, the SEM in the right column is the magnified image of the region in the white square in the SEM in the left column. The insets in the bottom left corners of (a), (c) and (e) are SEM images of silicon pyramids, original Klarite after gold being removed and silicon AFM tip before RIE treatment respectively. The orange scale bars in the insets in (a), (c) and (e) are 2 $\mu$ m, 1 $\mu$ m and 4 $\mu$ m in length respectively. The insets in the upper right corners of (b), (d) and (f) are photographs to compare the appearances of silicon pyramids (solar cell), silicon inverted pyramids (Klarite) and AFM tip chips with (black) and without (original) nanopillar forest. The scale bars in the insets in (b), (d) and (f) are 8cm, 1cm and 5mm respectively.

on the 3D microstructures. The insets on the upper right corners of Figure 1(b), (d) and (f) show the comparison of the appearances of these surfaces before and after being treated by our plasma etching process. We give the inverse silicon pyramids with slanted silicon nanopillar the name black Klarite. Both the positive pyramids and pyramidal pits are created by anisotropic chemical etching of silicon (100) plane so both contains exposed (111) planes with the angle of 54.7° with respect to the horizontal plane. [3] In this case, the angle of the incident plasma with the normal of the wall of pyramids is also 54.7°. For the AFM silicon cantilever tip case (Figure 1(e) (f)), we noticed that nanopillars are formed on most

<sup>1</sup>Micro and Nanotechnology Laboratory, University of Illinois at Urbana-Champaign, Urbana, IL 61801, USA (\*E-mail: [loganliu@illinois.edu](mailto:loganliu@illinois.edu))

surfaces only except of those surfaces that are too steep. This is prominent on Fig. 1(e), the side wall of the long sharp spike is almost vertical and they are smooth without any nanopillar. But on the tip of the spike that is a bit flat, the nanopillars are formed. This inspires us to investigate how the silicon nanopillar will be monolithically formed on surfaces with different slanted angles.

### III. ANGLE DEPENDENCE OF SLANTED NANOPILLAR

Figure 2 (a) is a cross-sectional SEM image of slanted pillar with slanted angle of 38°. The pillar slanted angle  $\beta$  is defined as the angle between the normal of silicon plane and the pillar. We tried etching angles  $\alpha$  of 0°, 8°, 15°, 20°, 30°, 40°, 50°, 60°, 70° respectively. As the etching angle  $\alpha$  increases, the pillar slanted angle  $\beta$  will also increase. But  $\beta$  is always smaller than  $\alpha$ . When the etching angle  $\alpha$  goes above 80°, the nanopillars will not form and thus the silicon substrate surface will not turn black. That explains why we did not obtain nanopillar structures on the nearly vertical sidewall of AFM tip in Fig. 1(e) and (f). The plot in Figure 2(b) shows the relationship of the etching angle  $\alpha$  and pillar slanted angle  $\beta$ .

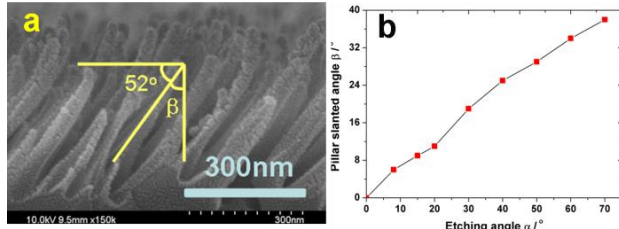


Figure 2 (a) cross-sectional SEM image of slanted pillar with slanted angle of 38°. (b) Relationship of the etching angle  $\alpha$  and pillar slanted angle  $\beta$ .

### IV. SERS MEASUREMENT

Figure 3(a) shows the SERS spectra of benzenethiol on smooth gold surface (black curve), original Klarite SERS substrate (green curve) and planar black silicon (red curve) and black Klarite (blue curve). The characteristic Raman peaks of benzenethiol are marked out at the wavenumber of 695 $\text{cm}^{-1}$  ( $\beta_{\text{CC}} + \nu_{\text{CS}}$ ), 1073 $\text{cm}^{-1}$  ( $\beta_{\text{CH}}$ ), 1575 $\text{cm}^{-1}$  ( $\nu_{\text{CC}}$ );  $\beta$  and  $\nu$  indicate the in-plane bending and the stretching modes respectively.[4] In Figure 3(a), the smooth gold surface hardly shows any Raman peaks while black Klarite and planar black silicon show higher peaks than original Klarite.

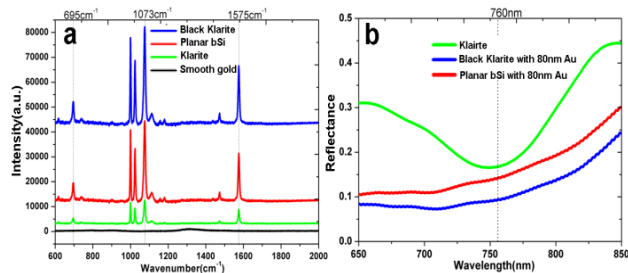


Figure 3. (a) Raman spectra of benzenethiol monolayer on different substrates including smooth gold surface (black), original Klarite SERS substrate (green), planar black silicon coated with 80nm Au (red) and black Klarite substrate coated with 80nm Au (blue). The exciting laser is with the

wavelength of 785nm, power of 1mW and exposure time of 10 seconds. (a.u.) stands for arbitrary units. (b) Reflection spectra of different substrates including original Klarite SERS substrate (green), planar black silicon coated with 80nm Au (red) and black Klarite substrate coated with 80nm Au (blue).

For a quantitative analysis of SERS enhancement, we calculated the enhancement factors of each substrate based on the peak intensity at 1073 $\text{cm}^{-1}$  since all the Raman peaks are proportional in intensity on each substrate. As original Klarite substrate is proved to have enhancement factor of  $\sim 10^6$ , [3] we use it as a reference to compute the enhancement factors for other substrates. The enhancement factor (EF) is calculated using the formula below:

$$EF = 10^6 \times \frac{I_{\text{specimen}}}{I_{\text{Klarite}}}, \quad (1)$$

In which  $10^6$  is the enhancement factor of original Klarite,  $I_{\text{specimen}}$  and  $I_{\text{Klarite}}$  are the Raman peak intensity at 1073 $\text{cm}^{-1}$  of the substrate of interest and original Klarite respectively. The calculated enhancement factors (EF) of different substrates are listed below:

TABLE I  
THE CALCULATED ENHANCEMENT FACTORS OF ORIGINAL KLARITE SERS SUBSTRATES, PLANAR BLACK SILICON AND BLACK KLARITE.

Substrate	Original Klarite	Planar blackSi	Black Klarite
EF	$1 \times 10^6$	$3.5 \times 10^6$	$3.9 \times 10^6$

### V. CONCLUSION

Nanopillar forest are formed on a variety of silicon surfaces with a 3-step self-masked reactive ion etching process. SERS enhancement factor of  $3.9 \times 10^6$  was achieved after depositing 80nm of gold onto Klarite SERS substrate we made black, compared with that of  $10^6$  of the original Klarite SERS substrate coated with 300nm of gold. Slanted nanopillar black silicon was produced with tilted etching process. The slanted nanopillar black silicon integrated on 3D microstructures provides new dimensions for fabrication and optimization of SERS sensors as well as other nanophotonic sensors.

### REFERENCES

- [1] I. Talian, K. B. Mogensen, A. Orinak, D. Kaniansky and J. Hubner, "Surface-enhanced Raman spectroscopy on novel black silicon-based nanostructured surfaces," *J. Raman Spectrosc.*, vol. 40, pp. 982-986, 2009.
- [2] Z. Xu, Y. Chen, M. R. Gartia, J. Jiang and G. L. Liu, "Surface plasmon enhanced broadband spectrophotometry on black silver substrates," *Appl. Phys. Lett.*, vol. 98, pp. 241904, 2011.
- [3] N. M. B. Perney, J. J. Baumberg, M. E. Zoorob, M. D. B. Charlton, S. Mahnkopf and C. M. Netti, "Tuning localized plasmons in nanostructured substrates for surface-enhanced Raman scattering," *Opt. Express*, vol. 14, pp. 857, 01/23, 2006.
- [4] R. L. Aggarwal, L. W. Farrar, E. D. Diebold and D. L. Polla, "Measurement of the absolute Raman scattering cross section of the 1584 $\text{cm}^{-1}$  band of benzenethiol and the surface-enhanced Raman scattering cross section enhancement factor for femtosecond laser-nanostructured substrates," *J. Raman Spectrosc.*, vol. 40, pp. 1331-1333, 2009.